Anal. Chem. **2003,** *75,* 3880−3889

Scanning Electrochemical Microscopy. 48. Hg/Pt Hemispherical Ultramicroelectrodes: Fabrication and Characterization

Janine Mauzeroll, Emily A. Hueske, and Allen J. Bard*

Department of Chemistry & Biochemistry, The University of Texas at Austin, Austin, Texas 78712

Hg/Pt hemispherical ultramicroelectrodes (UMEs) (25-*μ*m diameter) were prepared either by electrodeposition from a mercuric ion solution or by simple contact of the Pt disk to a hanging mercury drop electrode. The two methods produced equivalent tips. Optical inspection and electrochemical characterization of these Hg tips with methyl viologen, cobalt sepulchrate trichloride, and hexaaminеruthenium(III) chloride confirm the hemispherical nature of the UME. The scanning electrochemical microscopy approach curves for all three redox couples over a conductive substrate fit theoretical plots for hemispherical electrodes. The numerical solution of the diffusion equations for substrate generation−tip collection (SG-TC) transients for a finite Pt disk and Hg/Pt hemispherical UME are reported and compared to experimental results. A diffusion layer approximation is presented, and diffusion coefficients are extracted from the simulation. The SG-TC results reveal the enhanced sensitivity of hemispherical UME to radial diffusion.

We report the fabrication of Hg on Pt hemispherical scanning electrochemical microscopy (SECM) tips and their characterization. We also include experimental and theoretical comparison between substrate generation−tip collection (SG-TC) experiments at a Pt disk and Hg/Pt ultramicroelectrode (UME). Effects of tip-to-substrate separation were studied, and numerical analysis for both geometries correlated well with experimental results and allowed the extraction of diffusion coefficients. This study confirms the enhanced sensitivity of hemispherical tips to radial diffusion in SG-TC measurements and discusses the potential advantages of using such tips.

SECM transient current measurements provide information about homogeneous kinetics and time-dependent systems. The SECM transient response has previously been simulated and experimentally studied for planar electrodes, microdisks, and thin-layer cells over a wide time range.[1,2] Provided that the tip radius is known, transient current measurements allow for the determination of diffusion coefficients without knowledge of solution concentration and the number of electrons transferred.[3,4]

Most SECM investigations use Pt planar disk-shaped UMEs. However, for some studies, it is desirable to work at tip potentials in negative potential regions where proton reduction occurs at Pt. An example is the monitoring of Tl(I) as a surrogate for K(I) in studies of ion transport through channels in membranes[5,6] or in studies of surface reactions where a very negative redox couple, such as methyl viologen, is needed. Mandler and co-workers,[7] for example, demonstrated the use of an Hg−Au amalgam UME in SECM studies of surface reactions catalyzed by Pt.

There are a number of possible choices for the substrate for Hg UMEs. Ideally the substrate should be easily wet by mercury and yet have a low solubility in mercury. In the case of glassy carbon, the substrate surface shows poor wetting leading to the formation of inhomogeneous scattered mercury droplets.[8] For metals such as platinum, silver, and gold, the formation of intermetallic compounds at the base metal can occur. Thermal evaporation experiments have shown that the formation of intermetallic species leads to a potential window that extends to less negative potentials than that of the hanging mercury drop electrode (HMDE).[9] However, the dissolution of platinum is hindered by the presence of surface oxides and can often be neglected in voltammetric studies following the deposition of a sufficiently thick mercury layer.[10] Another possible substrate material is iridium. Osteryoung and co-workers fabricated and studied Ir-[11] and Ir/Pt[12] alloy-based mercury UMEs. However, the difficulty in obtaining Ir/Pt alloy wires in sufficiently small sizes and the brittleness of Ir wires make them less attractive as SECM probes. In this work, Pt was selected as the substrate.

Hg/Pt UMEs have a hemispherical shape. Conical-, hemispherical-, and spherical-shaped UMEs have been used in steady-state SECM studies, but little work has been done on the transient response of such tips.[13−18] Nonplanar UMEs are often easier to construct in small dimensions[19−22] and suffer less from problems with the insulating shielding hitting the substrate because of inexact alignment. This paper deals with the fabrication of

* Corresponding author. E-mail: ajbard@mail.utexas.edu.

(1) Bard, A. J., Mirkin, M. V., Eds. *Scanning Electrochemical Microscopy*; Marcel Dekker: New York, 2001.
(2) Bard, A. J.; Denuault, G.; Friesner, R. A.; Dornblaser, B. C.; Tuckerman, L. S. *Anal. Chem.* **1991**, *63*, 1282.
(3) Denault, G.; Mirkin, M. V.; Bard, A. J. *J. Electroanal. Chem.* **1991**, *308*, 27.
(4) Martin, R. D.; Unwin, P. R. *Anal. Chem.* **1998**, *70*, 276.
(5) Rueda, M.; Navarro, I.; Ramirez, G.; Prieto, F.; Prado, C.; Nelson, A. *Langmuir* **1999**, *15*, 3672.
(6) Mauzeroll, J.; Buda, M.; Bard, A. J.; Prieto, F.; Rueda, M. *Langmuir* **2002**, *18*, 9453.
(7) Selzer, Y.; Turyan, I.; Mandler, D. *J. Phys. Chem. B* **1999**, *103*, 1509.
(8) Wu. H. P. *Anal. Chem.* **1994**, *66*, 3151.
(9) Yoshima, Z. *Bull. Chem. Soc. Jpn.* **1981**, *54*, 556.
(10) Wehmeyer, K. R.; Wightman, R. M. *Anal. Chem.* **1985**, *57*, 1989.
(11) Golas, J.; Galus, Z.; Osteryoung, J. *Anal. Chem.* **1987**, *59*, 389.
(12) Wechter, C.; Osteryoung, J. *Anal. Chim. Acta* **1990**, *234*, 275.

10.1021/ac034088l CCC: $25.00
Published on Web 06/24/2003

hemispherical tips, their characterization, and their application in substrate generation−tip collection SECM studies. In SG-TC SECM mode, the substrate electrogenerates a species that diffuses into the bulk. A UME positioned close to the substrate collects the generated species. The tip is at least 1 order of magnitude smaller than the substrate and has a thinner diffusion layer than the substrate. The tip reaction, therefore, does not significantly affect the substrate current except at very small separations.

Historically, SG-TC experiments with an amperometric tip were pioneered by Engstrom et al.[23−25] Using small carbon UMEs, they collected and studied species generated at a close macroscopic electrode. They addressed the theoretical behavior of the tip transient response using potential step functions and impulse response functions. Other mathematical approaches have been applied to the theory of a disk-shaped tip and flat substrate, including finite element,[26] boundary element,[27] and alternating direction implicit finite difference methods (ADIFDM).[28] Selzer and Mandler[17] recently treated the theoretical behavior of a hemispherical UME used in feedback SECM studies by ADIFDM and compared these simulations to those previously obtained by the same method for a finite disk. Here, we follow this theoretical comparison with experimental characterization of a hemispherical mercury UME by SECM in the SG-TC mode and numerical simulations based on the finite element method (FEM).

EXPERIMENTAL SECTION

Electrodes. A 25-μm-diameter Pt wire (Goodfellow, Cambridge, U.K.) was sealed into a 5-cm Pyrex glass capillary under vacuum as described previously.[2] The electrode was polished and shaped into a UME on a polishing wheel (Buehler, Lake Bluff, IL) with 180-grid Carbimet paper disks (Buehler) and micropolishing cloth with 1.0-, 0.3-, and 0.05-μm alumina (Buehler). The tip was sharpened to an RG of 2−3, where RG is the ratio of the diameter of the UME that includes the glass sheet and the diameter of the Pt wire.

Hemispherical Hg/Pt UMEs were produced using two equivalent methods. Mercury was deposited onto the Pt UME from a 10 mM $Hg_2(NO_3)_2$ (J. T. Baker Chemical Co. Phillipsburg, NJ) in 0.1 M KNO_3 solution acidified to 0.5% with HNO_3 in a three-electrode setup and controlled by a model 660 potentiostat (CH Instruments, Austin, TX). A 1-mm Pt wire served as a counter electrode, and a fritted Ag/AgCl electrode served as a reference electrode. The working Pt UME and counter electrode were inserted through a hole at the base of the cell while the reference was positioned in a side compartment as seen in Figure 1. The deposition curve was recorded during a 300-s potential step of −0.1 V versus Ag/AgCl. The deposition was monitored in situ with an optical microscope (Olympus model BH-2) equipped with a water immersion objective (Olympus FLxw40). A personal computer and Pixera camera (PVC 100c, Pixera Corp.) were used to record the images. The voltammetric characterization and feedback SECM studies of the Hg/Pt UME presented in this paper used this first method.

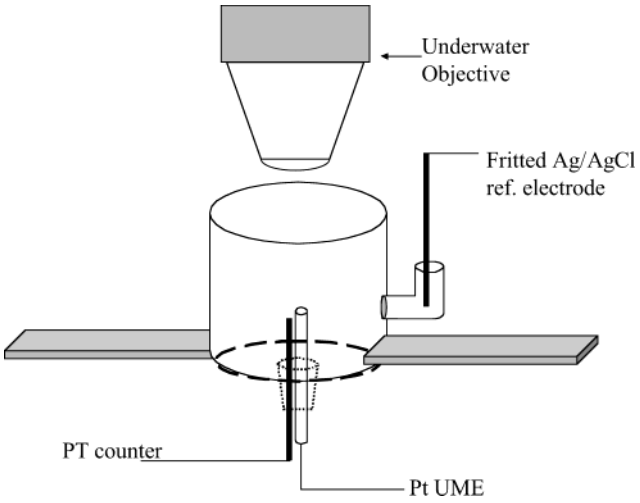

Figure 1. Experimental setup for the formation of Hg/Pt UME by electrodeposition from a $Hg_2(NO_3)_2$ solution with 0.1 M KNO_3 acidified to 0.5% with HNO_3 as supporting electrolyte. This glass cell was joined at the base with a microscope slide. The underwater objective was lowered into solution, and the deposition curve recorded during a 300-s potential step of −0.1 V vs Ag/AgCl.

In a second method to produce the Hg/Pt UME, the Pt UME was sealed into a J glass tube using Teflon tape to give a submarine electrode.[29] The Hg/Pt UME was then formed by applying −1.1 (V vs Hg/Hg_2SO_4 (Radiometer, Copenhagen, Denmark)) at the Pt UME and contacting it with the mercury (Bethlehem Instruments, Hellertown, PA) of a hanging mercury drop electrode (Metrohm Instruments, Herisau, Switzerland) in phosphate buffer. Reproduction of the voltammetric and SECM characterization confirmed that the two methods used to form Hg/Pt electrodes were equivalent. The SG-TC experiments were performed with UME produced by this second method.

Materials and Solutions. Cyclic voltammetry and SECM characterization experiments used concentrations of 1 mM in cobalt sepulchrate trichloride (Aldrich), hexaminerutheniu(III) chloride (Strem Chemicals, Newbury Port, MA), methyl viologen (Aldrich) redox couples. The supporting electrolyte used for the SG-TC experiments is formed by 0.1 M KCl solutions buffered by a 1:1 molar ratio of NaH_2PO_4/Na_2HPO_4 of total concentration of 0.01 M at pH 7. The redox couples employed are 1 mM hexaminerutheniu(III) chloride (Strem Chemicals) and thallium-(I) nitrate (Aldrich). The stock solution of 0.1 M thallium nitrate

(13) Mirkin, M. V.; Fan, F.-R. F.; Bard, A. J. *J. Electroanal. Chem.* **1992**, *328*, 47.
(14) Demaille, C.; Brust, M.; Tionsky, M.; Bard, A. J. *Anal. Chem.* **1997**, *69*, 2323.
(15) Fulian, Q.; Fisher, A. C.; Denuault, G. *J. Phys. Chem. B* **1999**, *103*, 4387.
(16) Fulian, Q.; Fisher, A. C.; Denuault, G. *J. Phys. Chem. B* **1999**, *103*, 4393.
(17) Selzer, Y.; Mandler, D. *Anal. Chem.* **2000**, *72*, 2383.
(18) Zoski, C. G.; Mirkin, M. V. *Anal. Chem.* **2002**, *74*, 1986.
(19) Fan, F.-R. F.; Bard, A. J. *Science* **1995**, *267*, 871.
(20) Fan, F.-R. F.; Bard, A. J. *Science* **1995**, *270*, 1849.
(21) Fan, F.-R. F.; Bard, A. J. *Proc. Natl. Acad. Sci. U.S.A.* **1999**, *96*, 14222.
(22) Gray, N. J.; Unwin, P. R. *Analyst* **2000**, *125*, 889.
(23) Engstrom, R. C.; Weber, M.; Wunder, D. J.; Burgess, R.; Winquist, S. *Anal. Chem.* **1986**, *58*, 844.
(24) Engstrom, R. C.; Meaney, T.; Tople, R.; Wightman, R. M. *Anal. Chem.* **1987**, *59*, 2005.
(25) Engstrom, R. C.; Wightman, R. M.; Kristensen, E. W. *Anal. Chem.* **1988**, *60*, 652.
(26) Kwak, J.; Bard, A. J. *Anal. Chem.* **1989**, *61*, 1221.
(27) Fulian, Q.; Fisher, A. C.; Dennuault, G. *J. Phys. Chem. B* **1999**, *103*, 4393.
(28) Unwin, P. R. *J. Chem. Soc., Faraday Trans.* **1998**, *94*, 3183.
(29) Slevin, C. J.; Umbers, J. A.; Atherton, J. H.; Unwin, P. R. *J. Chem. Soc., Faraday Trans.* **1996**, *92*, 5177.

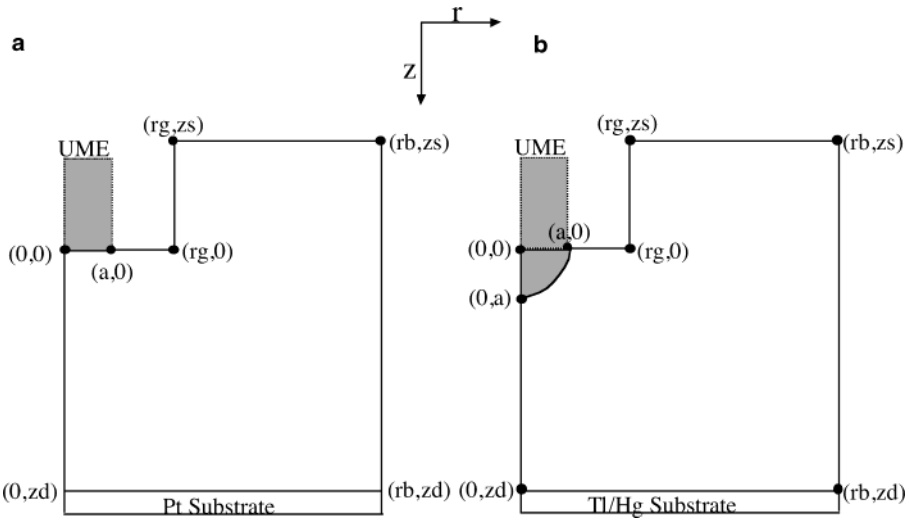

Figure 2. Defined space domain for the numerical analysis of (a) finite planar disk and (b) hemispherical UME.

was made in water. The thallium concentration in the reaction cell was 10^{-4} M. All solutions were prepared with Milli-Q (Millipore Corp.) reagent water and degassed with Ar for 30 min prior to all experiments.

SECM Apparatus. A CHI model 900 scanning electrochemical microscope (CH Instruments, Austin, TX) was used to control the tip potentials, obtain the approach curves, and monitor the tip-to-substrate distance. A home-built floating potentiostat was used to control the HMDE or Pt disk substrate potential. The use of this battery-operated potentiostat as the potential control for the substrate prevented interferences observed with the CHI instrument during transient measurements when the tip was positioned in close proximity to the substrate.

The cell platform was modified to accommodate a chamber designed to allow measurements under oxygen-free conditions. In the case of the Tl collection experiment, the experimental setup has been described elsewhere.[6] As for the other SECM experiments, they were performed either with the SECM head in a glovebag under positive pressure or the SECM cell covered with Parafilm and in the presence of an argon blanket.

SG-TC Experiments. The SG-TC experiments at a disk electrode were performed in a Teflon SECM cell that accommodated four electrodes. The Pt disk UME approached the Pt substrate in the feedback mode. The tip was positioned close to the substrate, and the tip current transient response for different tip-to-substrate separations was measured. For each tip-to-substrate separation, a new solution containing redox species was added. At the end of the experiment, an approach curve was measured to evaluate the true tip-to-substrate distance based on an SECM calibration.

The SG-TC experiments at the Hg/Pt UME were performed in a 750-mL cut beaker with a machined Teflon cap with an O-ring. The cap accommodated the HMDE, the submarine electrode, a reference electrode, an auxiliary electrode, a gas inlet, and a microsyringe. An argon blanket was maintained over the solution at all times.

The reaction vessel was filled with 250 mL of phosphate buffer and closed with all electrodes in place. The solution was purged with argon for 30 min. The tip and HMDE (area, $A = 0.0139 \pm 0.0003$ cm^2) were aligned during the formation of the Hg/Pt UME. The tip was then retracted from the HMDE to a known distance. The reaction vessel was deaerated for 30 min after which 250 mL of $TlNO_3$ stock solution was added. Voltammetric response of thallium ion was then recorded at both tip and substrate.

The distance dependence of the tip transient response was evaluated. The substrate and the tip were both poised at −1.1 V for 30 s to respectively form the substrate amalgam and stabilize the tip current. The substrate potential was then switched to −0.75 V to oxidize the thallium amalgam. The tip collected the released thallium ions from the substrate for 100 s and remained poised at −1.1 V. The tip was then moved 25 mm further away from the substrate, and the experiment was repeated for several tip-to-substrate distances. A new amalgamated HMDE was used for each distance. Upon completion, an approach curve was recorded to assess the true tip-to-substrate distance.

RESULTS AND DISCUSSION

Numerical Simulation of SG-TC Mode for Disk and Hemispherical UME. In SG-TC experiments, the substrate electrogenerates redox-active species, R, from an initial solution of species, O. The generated R diffuses away from the substrate, and a fraction is collected at the nearby UME and undergoes the reverse reaction, oxidation to O. The tip response varies with time and depends on the tip geometry, the tip-to-substrate separation, and the concentration profile generated at both the substrate and tip.

The concentration of a species, I, is denoted as $C_i(r,z,t)$ and the diffusion equation for that species in cylindrical coordinates is

$$\frac{\partial C_i}{\partial t} = D_i\left(\frac{\partial^2 C_i}{\partial r^2} + \frac{1}{r}\frac{\partial C_i}{\partial r} + \frac{\partial^2 C_i}{\partial z^2}\right) \qquad (1)$$

where r and z are radial and normal directions from the tip surface, D_i is the diffusion coefficient of i, C_i is the concentration of the species (O or R), and t is the time.

In the present experiments, the initial and boundary conditions for the planar disk and the hemispherical UME are different as a

result of the redox couple used for each UME and the geometry of the tip. The planar disk SG-TC experiment involved both O and R soluble and, hence, concentration profiles of both the Ru(II) and Ru(III) species. Thus, two diffusion equations were solved simultaneously and the boundary conditions for both species were defined. The hemispherical UME SG-TC experiment involved only one electroactive species soluble in the aqueous medium, Tl(I), and required the solution of only one partial differential equation. The initial and mixed boundary conditions for both experiments were defined at every line of the domains in Figure 2. For each tip geometry, the initial and mixed boundary conditions are as follows:

planar disk

$$t = 0; \quad C_o = C_o^*; \quad C_R = 0 \tag{2}$$

$$t > 0; r = 0; \quad 0 \le z \le \mathrm{zd}; \quad \frac{\partial C_o}{\partial r} = \frac{\partial C_R}{\partial r} = 0 \tag{3}$$

$$t > 0; \quad 0 \le r \le \mathrm{rb}; \quad z = \mathrm{zd}; \quad C_o = 0; \quad C_R = C_o^* \tag{4}$$

$$t > 0; \quad r = \mathrm{rb}; \quad \mathrm{zs} \le z \le \mathrm{zd}; \quad \frac{\partial C_o}{\partial r} = \frac{\partial C_R}{\partial r} = 0 \tag{5}$$

$$t > 0; \quad \mathrm{rg} \le r \le \mathrm{rb}; \quad z = \mathrm{zs}; \quad C_o = C_o^*; \quad C_R = 0 \tag{6}$$

$$t > 0; \quad r = \mathrm{rg}; \quad \mathrm{zs} \le z \le 0; \quad \frac{\partial C_o}{\partial r} = \frac{\partial C_R}{\partial r} = 0 \tag{7}$$

$$t > 0; \quad a \le r \le \mathrm{rg}; \quad z = 0; \quad \frac{\partial C_o}{\partial z} = \frac{\partial C_R}{\partial z} = 0 \tag{8}$$

$$t > 0; \quad 0 \le r \le a; \quad z = 0; C_o = C_o^*; \quad C_R = 0 \tag{9}$$

hemisphere

$$t = 0; \quad C_o = C_o^* \tag{10}$$

$$t > 0; \quad r = 0; \quad a \le z \le \mathrm{zd}; \quad \frac{\partial C_o}{\partial r} = 0 \tag{11}$$

$$t > 0; \quad 0 \le r \le \mathrm{rb}; \quad z = \mathrm{zd}; \quad C_o = C_{\mathrm{amal}}^* \tag{12}$$

$$t > 0; \quad r = \mathrm{rb}; \quad \mathrm{zs} \le z \le \mathrm{zd}; \quad \frac{\partial C_o}{\partial r} = 0 \tag{13}$$

$$t > 0; \quad \mathrm{rg} \le r \le \mathrm{rb}; \quad z = \mathrm{zs}; \quad C_o = C_o^* \tag{14}$$

$$t > 0; \quad r = \mathrm{rg}; \quad \mathrm{zs} \le z \le 0; \quad \frac{\partial C_o}{\partial r} = 0 \tag{15}$$

$$t > 0; \quad a \le r \le \mathrm{rg}; \quad z = 0; \quad \frac{\partial C_o}{\partial z} = 0 \tag{16}$$

$$t > 0; \quad 0 \le r \le a; \quad z = (\mathrm{a}^2 - r^2)^{1/2}; \quad C_o = 0 \tag{17}$$

where t is the time, a is the radius of the Pt wire, rg is the radius of the UME that includes the glass sheet, zs an arbitrary distance above the tip bottom that is large compared to the substrate diffusion layer, rb is the substrate radius, and zd is the tip-to-substrate separation distance.

The tip transient response was simulated using an FEM. This method differs from difference methods because it is based on a discretized polynomial approach. It is useful because it can be applied to any geometrical shape and has been well-documented in previous electrochemical studies.[26,30−34] In the FEM, the concentration gradient of species is approximated using a sequentially continuous function. In our case, a 2D grid is defined with triangular elements. At each node, basis functions, usually linear and quadratic polynomials, are defined to ensure continuity. Space and time matrixes are then solved numerically. To calculate the tip current, the concentration gradient normal to the tip surface is approximated. Taking advantage of the symmetry of the defined spaces in Figure 2a, the tip current is then

$$i_{\mathrm{tip}} = nFD\left\{\int_{r=0}^{r=a} 2\pi r \left(\frac{\partial C_i}{\partial z}\right)_{z\cong 0} \mathrm{d}r\right\} \tag{18}$$

A similar integration was performed for the hemispherical geometry along the arc as defined in Figure 2b. All these calculations were carried out with PDEase2D (Macsyma Inc., Arlington, MA), a commercial program that employs the FEM.[35]

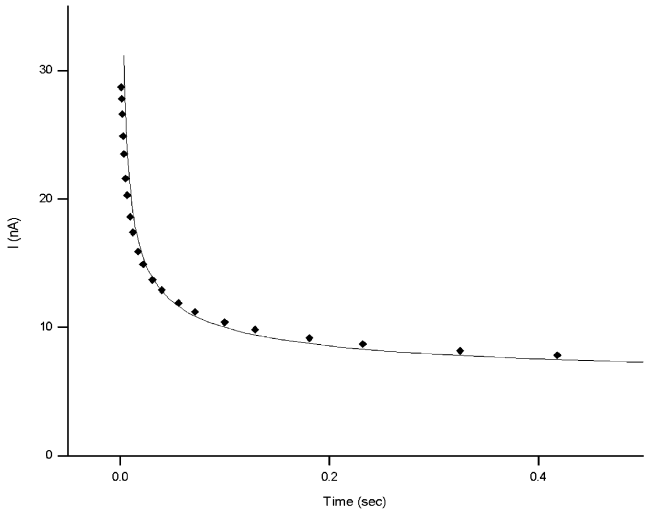

Figure 3. Fitting of the numerical simulation results for a large-amplitude potential step at a 25-μm UME to the equation of Shoup and Szabo.[36] This fitting was done for a tip in a 1 mM $Ru(NH_3)_6Cl_3$ solution with a diffusion coefficient of 6.7×10^{-6} cm^2/s.

SG/TC Experiments at a Disk UME. The numerical simulation for the disk UME response to a large-amplitude potential step in bulk solution was examined to test the simulation when compared to known theory. Initially, the UME is at a potential where O is not reduced. The application of a potential step at $t = 0$ causes reduction of O at a diffusion-controlled rate. The diffusion to a planar disk UME occurs in two dimensions. This implies that the current density is not uniform across the disk, and this was observed in the simulations. The simulated current response was compared to the expression given by Shoup and Szabo:[36]

(30) Penczek, M.; Stojek, Z. *J. Electroanal. Chem.* **1984**, *170*, 99.
(31) Penczek, M.; Stojek, Z. *J. Electroanal. Chem.* **1984**, *181*, 83.
(32) Moorhead, E. D.; Stephens, M. M. *J. Electroanal. Chem.* **1990**, *282*, 1.
(33) Nann, T.; Heinze, J. *Electrochem. Commun.* **1999**, *1*, 289.
(34) Lee, Y.; Amemiya, S.; Bard, A. J. *Anal. Chem.* **2001**, *73*, 2261.
(35) Mirkin, M. V. In *Scanning Electrochemical Microscopy*; Bard, A. J., Mirkin, M. V., Eds.; Marcel Dekker: New York, 2001; Chapter 4.
(36) Shoup, D.; Szabo, A. *J. Electroanal. Chem.* **1982**, *140*, 237.

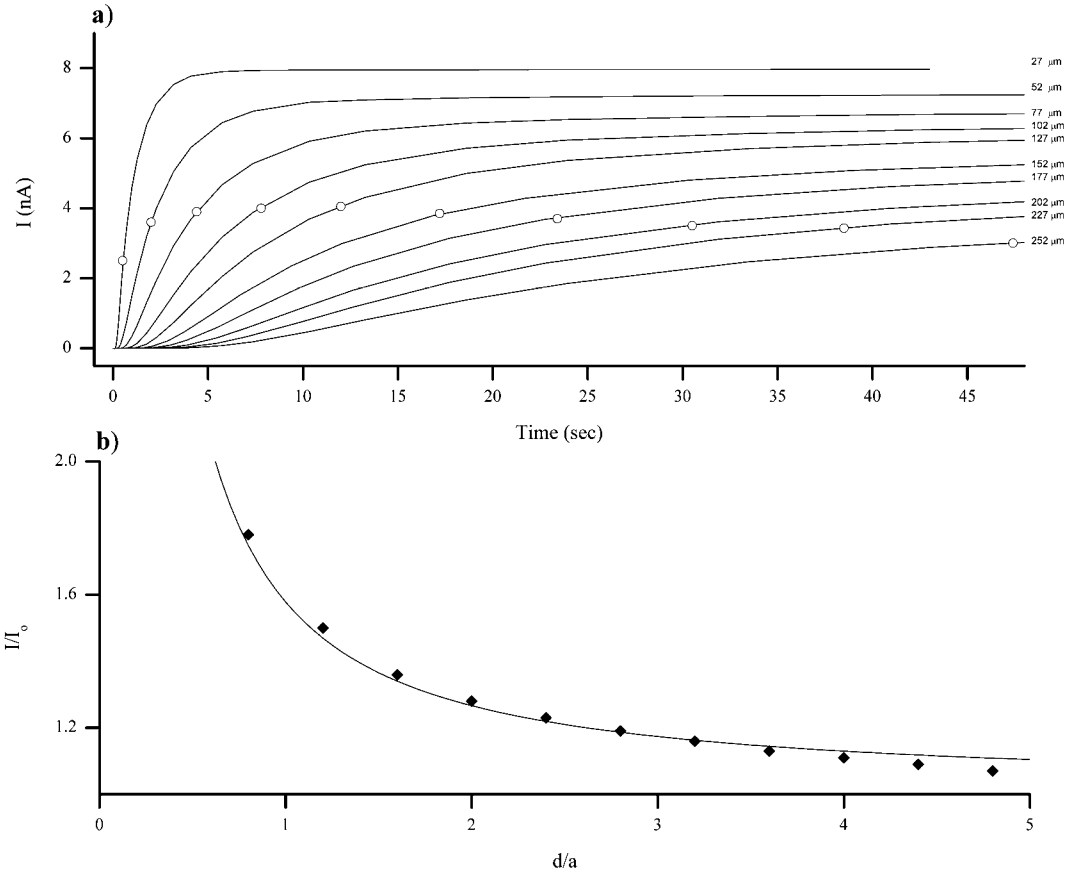

Figure 4. (a) SG-TC simulation at a finite disk for different tip-to-substrate separations for a 25-μm UME tip in a 1 mM $Ru(NH_3)_6Cl_3$ solution with an assumed diffusion coefficient of 6.7×10^{-6} cm^2/s. (o) Diffusion time calculated from the diffusion layer thickness approximation: $\delta = \sqrt{(2Dt)}$. (b) Fitting of the simulated steady current for different tip-to-substrate separations and positive feedback SECM theory for a finite disk.

$$i_{tip} = \frac{4nFAD_oC_o^*}{pa}\{0.7854 + 0.8862\tau^{-1/2} + 0.2146e^{-0.7823\tau^{-1/2}}\} \quad (19)$$

where $\tau = 4D_0t/a^2$, F is Faraday's constant (96487 C/equiv), n is the number of electrons (equiv/mol), A is the area of the disk (cm^2), D_0 is the diffusion coefficient (cm^2/s), C_0* is the bulk concentration of O (mol/cm^3), and a is the radius of the disk UME (cm).

Equation 19 describes the chronoamperometric behavior of a finite disk electrode and improved on Osteryoung and Aoki's previous work that separated the response into two time ranges where different series were applicable.[37] Shoup and Szabo's relationship showed good correlation between experimental results and digital simulations that were based on an explicit hopscotch algorithm. The results of our numerical simulation in Figure 3 also produced a good correlation with eq 19. The numerical simulation and theory were computed for the chronoamperometric behavior of a 25-μm Pt tip in a 1 mM $Ru(NH_3)_6^{3+}$Ru(III) quiescent solution with a diffusion coefficient of 6.7×10^{-6} cm^2/s.

The same conditions were used in the SG-TC simulation at a finite planar disk for different tip-to-substrate separations as presented in Figure 4a. As the tip was moved further away from the generating substrate, the steady-state current decreased. Previous simulations have used the decrease in steady-state current to test their simulations to SECM feedback theory.[4,38] The normalized steady-state current for a conductive approach curve is given by

$$i_t/i_{t,\infty} = 0.68 + 0.7838/L + 0.3315\exp[-1.0672/L] \quad (20)$$

where i_t is the tip current, $i_{t,\infty}$ is the steady-state current when the tip is far from the substrate, and L is the ratio of the tip-to-substrate spacing and the tip radius (12.5 μm). As seen from Figure 4b, the steady-state currents obtained from the simulation at different tip-to-substrate separations fit SECM theory well.

At small tip-to-substrate distances, the rising transient response has a steeper slope and a shorter diffusion time as shown in Figure 4a. As the separation increases, the slope of the transient decreases, and the diffusion time increases. The diffusion layer thickness is often approximated by

$$\delta = \sqrt{2Dt} \quad (21)$$

where D is the diffusion coefficient (cm^2/s), t is the time (s) and δ is the thickness of the diffusion layer (cm). This approximation yields the diffusion times shown as circles in Figure 4a. From the simulation, one notes that the detection of current occurs sooner and suggests that, in experimental measurements, eq 21 is not a good approximation to estimate the tip-to-substrate separation.

(37) Aoki, K.; Osteryoung, J. *J. Electroanal. Chem.* **1981**, *122*, 19.

(38) Martin, R. D.; Unwin, P. R. *J. Electroanal. Chem.* **1997**, *439*, 123.

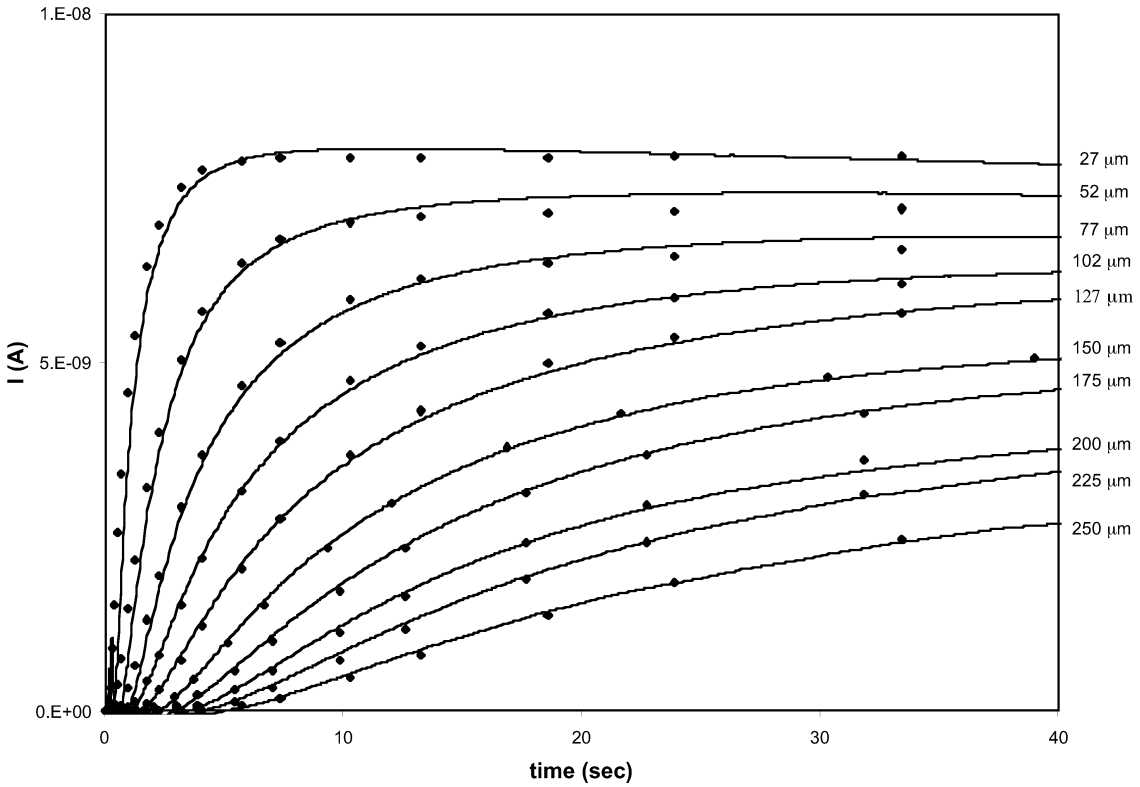

Figure 5. One-parameter fit of the simulated and experimental results for the SG-TC of 1 mM $Ru(NH_3)_6Cl_3$ solution at a 25-μm Pt finite disk UME for different tip-to-substrate distances and a diffusion coefficient of 6.7×10^{-6} cm^2/s.

The results for the SG-TC experiments at a planar disk UME are presented in Figure 5. In this experiment, a large Pt substrate electrogenerated $Ru(NH_3)_6^{2+}$ from an initial solution containing $Ru(NH_3)_6^{3+}$. A fraction of the generated +2 species diffuses from the substrate and is then intercepted by the 25-μm Pt disk UME, causing an increase in tip current. The tip current eventually reaches a quasi steady state, when the concentration of +2 at the tip approaches the original bulk concentration of $Ru(NH_3)_6^{3+}$. The tip-to-substrate separation affects the diffusion time, the fraction of $Ru(NH_3)_6^{2+}$ that is collected at the tip, and the magnitude of the steady-state tip current. The experiment was repeated for several tip-to-substrate separations, x, which were evaluated from an SECM calibration based on a feedback approach curve. From Figure 5, we see that the smaller was x, the steeper the slope of the transient response, the shorter the diffusion time, and the larger the final steady-state current. This behavior is consistent with that reported by Martin and Unwin for smaller tip-to-substrate separations.[4] At longer times then those shown here, convection occurred and caused the current to decrease.

In fact, the simulated data, as shown in Figure 5, fit the experimental results quite well. In the simulation, the diffusion coefficients of reduced and oxidized species are assumed to be the same. The diffusion coefficient extracted from the simulation ($D_s = 8.7 \times 10^{-6}$ cm^2/s) is also in good agreement with the experimental one ($D = 6.7 \times 10^{-6}$ cm^2/s).

Engstrom et al. suggested using an error function complement approximation in earlier work.[23] They showed that the general shape, amplitude, and time delay of the erfc predicted their experimental results for tip-to-substrate spacing greater than 10 μm. The concentration profile of the generated species, $C_o(x,t)$, was treated as a double potential step chronoamperometric problem.[6] The concentration profile generated at the substrate and detected by tip is given by[39]

$$C_o(x,t) = C_o^* \text{ erfc}[x/2(D_0t)^{1/2}] \qquad (22)$$

where C_o^* is the bulk concentration of the species in solution before electrolysis, x is the tip-to-substrate distance, and t is time.

Table 1. Tip-to-Substrate Distance Evaluation Using an Error Function Complement Approximation[a]

erfc argument	x_{erfc} (μm)	x_{SECM} (μm)
0.643	33	27
1.005	52	52
1.795	92	77
2.129	110	102
2.546	131	127
2.991	154	152
3.362	174	177
3.770	195	202
4.192	217	227
4.648	240	252

[a] From the error function complement argument, the tip-to-substrate distance is extracted and compared to the distance obtained by the experimental approach curve fitting to hemispherical SECM theory. The collection transient responses at the tip were fitted to the error function complement approximation. From the error function complement argument, the tip-to-substrate distance (x) was extracted and compared to the tip-to-substrate distances evaluated from the SECM calibration.

(39) Bard, A. J.; Faulkner, L. R. *Electrochemical Methods*, 1st ed.; John Wiley & Sons: New York, 1980; p 180.

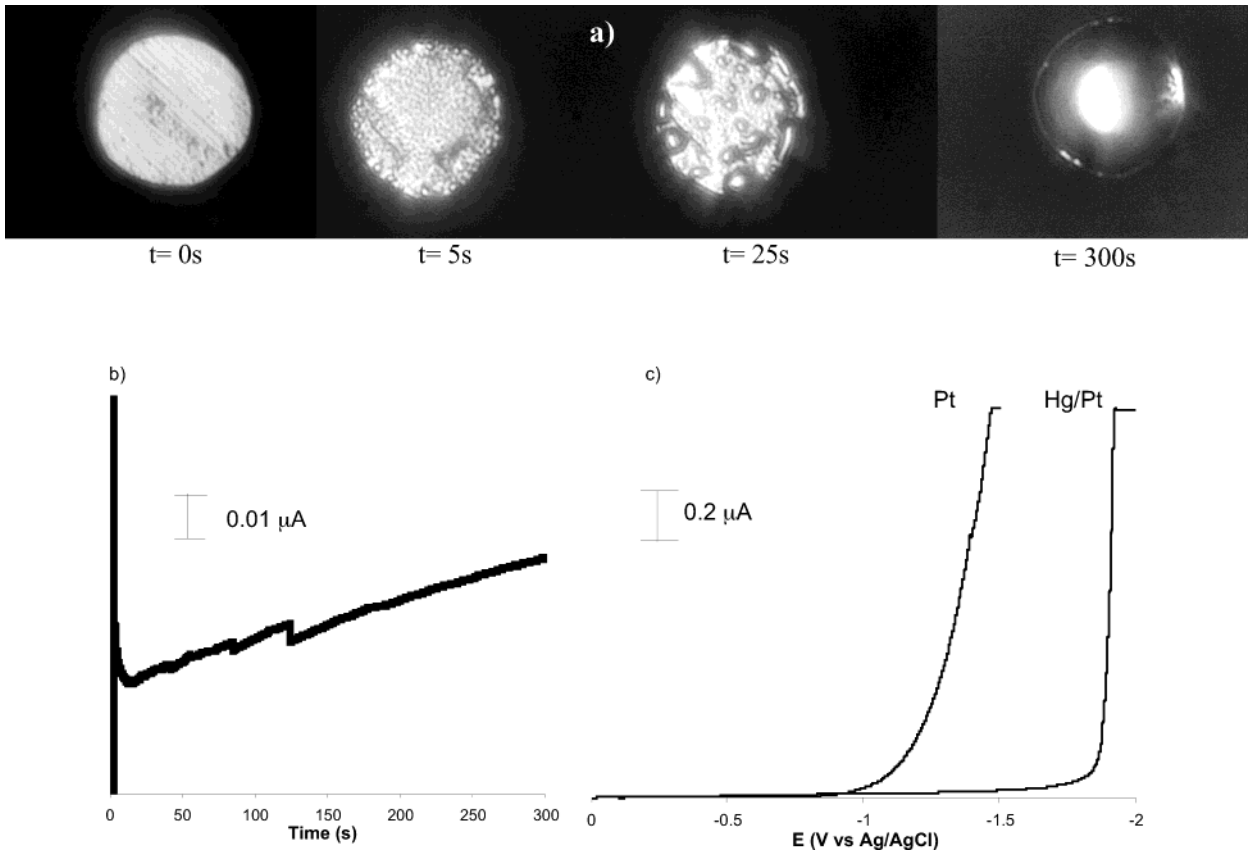

Figure 6. Characterization of the 25-μm Hg/Pt UME. (a) In situ micrographs of mercury deposition (0−300 s) from a 10 mM $Hg_2(NO_3)_2$ solution with 0.1 M KNO_3 supporting electrolyte acidified to 0.5% with HNO_3. (b) The deposition curve recorded during a 300-s potential step of −0.1 V vs Ag/AgCl. A 1-mm Pt wire served as counter electrode, and a fritted Ag/AgCl electrode served as reference electrode. (c) Current−potential curves at Pt and Hg/Pt UMEs in 0.1 M KNO_3.

Equation 22 expresses the concentration as a function of t at a given distance and can be substituted in eq 23 to yield a tip current expression that also depends on time and tip separation.

$$i_T = 4nFDC_o(x,t)a \qquad (23)$$

The best fit values of x of the data in Figure 5, which is reported in Table 1, are then obtained by fitting eq 23 to the data in Figure 5. These values are compared to the distances evaluated from the steady-state SECM feedback approach curves. At smaller distances, the approximation in eq 22 does not hold as well because of feedback effects. At intermediate-to-long distances, however, a better agreement with the SECM-derived distances is observed.

Formation and Characterization of a Hg/Pt UME. Mercury Deposition. We now discuss the fabrication of a Hg/Pt tip and its use in the SECM. As discussed in the Experimental Section, Hg is electrodeposited on the planar Pt UME disk. In the first stages of deposition, a very thin layer of intermetallic species (Pt_2Hg) is formed.[9] This is followed by the spontaneous formation of mercury nuclei (Figure 6a) close to the edge of the platinum/glass interface where the current density is the highest.[40] With time, the nuclei coalesce until a full hemisphere is formed. This coalescence alters the surface area of the electrode and leads to indentations in the current deposition curves (Figure 6b). These results are consistent with previously reported work.[11] Once formed, the mercury hemisphere is firmly attached to the platinum substrate and could withstand washing; however, it could not be stored in air and left to dry. When dry, the hemisphere shrank and sometimes exposed platinum as a result of surface tension changes. Hg UMEs were therefore stored in a degassed potassium nitrate solution.

Voltammetry. The electrochemical behavior and stability of the Hg UME was evaluated using linear sweep voltammetry. After mercury deposition, the proton reduction overpotential shifted to more negative potentials from that seen at bare Pt by ~800 mV (Figure 6c). Dirty or damaged electrodes only shifted the overpotential by ~200 mV and showed prewaves characteristic of platinum microarrays. Clean UMEs with a thick mercury deposit, however, were well behaved.

Proton reduction at Pt is catalyzed by methyl viologen. Electrochemical studies of this couple in aqueous media must therefore be performed at a mercury electrode. The methyl viologen voltammogram at the Hg UME was well behaved (Figure 7a), confirming good coverage of the Pt disk and demonstrating the use of Hg UMEs as probes in SECM in the negative potential regime.

The geometry of the Hg tip was confirmed by the change in limiting current in voltammograms of $Ru(NH_3)_6^{3+}$ (Figure 7a). The

(40) Sharifer, B.; Hills, G. J. *J. Electroanal. Chem.* **1981**, *130*, 81.

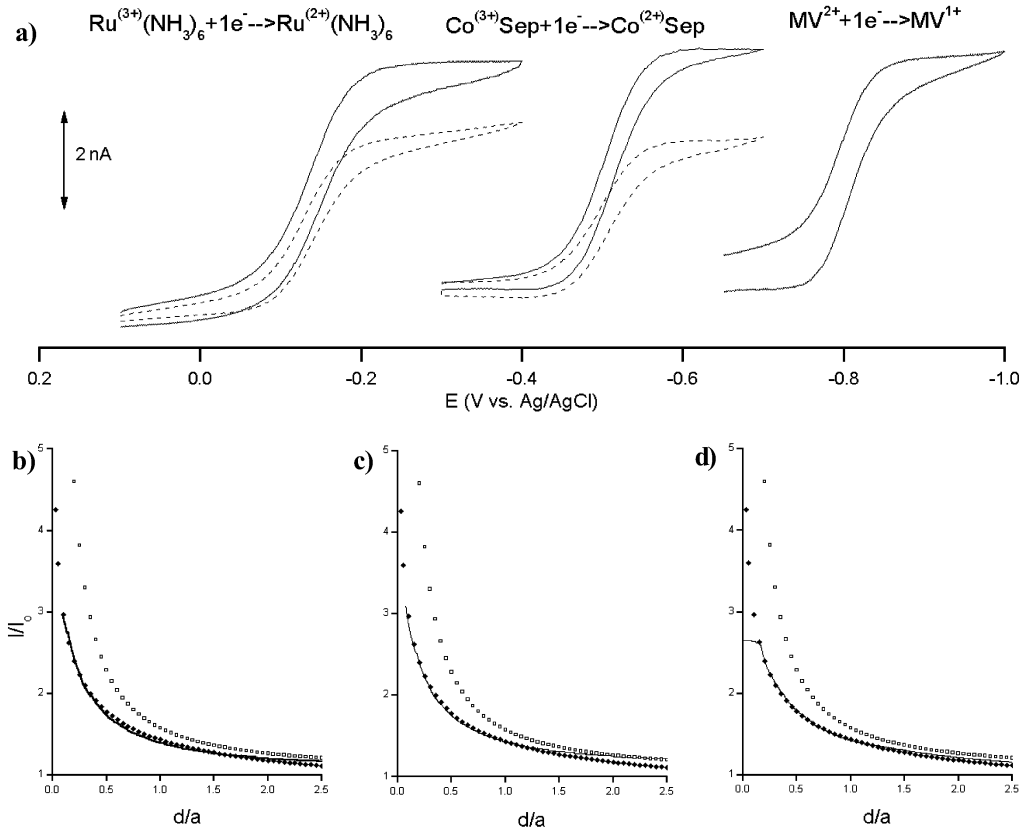

Figure 7. (a) Voltammetric behavior of the 25-μm (- - -) Pt and (—) Hg/Pt UMEs in 1 mM $Ru(NH_3)_6Cl_3$, cobalt sepulchrate trichloride and methyl viologen in 0.1 M KNO_3. (b) Positive feedback SECM fitting of the (□) finite disk theory, (◆) hemispherical disk theory, and (line) experimental results for the 1 mM $Ru(NH_3)_6Cl_3$. (c) Positive feedback SECM fitting of the (□) finite disk theory, (◆) hemispherical disk theory, and (line) experimental results for the 1 mM cobalt sepulchrate trichloride in 0.1 M KNO_3. (d) Positive feedback SECM fitting of the (□) finite disk theory, (◆) hemispherical disk theory, and (line) experimental results for the 1 mM methyl viologen.

voltammograms showed a wave at the standard potential of the couple and a stable steady-state current. An increase in steady-state current was observed for the Hg UME relative to the Pt UME because of the change in geometry from disk to hemisphere. This follows the theoretical equations of the steady-state current at microelectrodes where the ratio of the limiting current of a disk UME[41] and that of a hemispherical UME is close to $\pi/2$. The observed change of steady-state current (i_h/i_d = 1.47) from the Pt UME to the Hg UME is close to this value for $Ru(NH_3)_6^{3+}$, confirming the near-hemispherical geometry of the UME. The radius (r_{exp} = 12.6 μm), calculated from the voltammogram, is also equal to that of the mirodisk. A similar increase in the steady-state ratio (i_h/i_d = 1.57) was observed for cobalt sepulchrate trichloride (Figure 7a). Thus, both the optical and voltammetric analysis confirm the hemispherical geometry of the UME.

SECM Experiments with the Hg/Pt Tip in the Feedback Mode. The theory[26,42,43] and applications of SECM have been discussed elsewhere.[35] Relevant to the present measurements is the effect of tip geometry on the SECM approach curves. An approximate approach to this question treated different tip shapes, e.g., cones and hemispheres, as variations on a collection of disks.[13] The shape of the hemispherical approach curve demonstrates the reduced sensitivity of the mercury electrode to feedback relative to the Pt disk electrode (Figure 7b–d). This agrees with previously reported studies of gold spherical ultramicroelectrodes prepared by self-assembly of gold nanoparticles.[14] The diffusion of the electroactive species normal to the disk UME outweighs the radial diffusion component as the tip approaches a conductive substrate. The theoretical approach curve for a hemisphere, therefore, demonstrates the lower sensitivity inherent to the geometry of the tip. As the tip approaches the conductive substrate, the current measured will systematically be inferior to that measured at the disk electrode. Based on Figure 7b–d, all three tested redox couples present this behavior and are consistent with the theoretical current expression of Mandler et al.[7]

Experimentally, the close approach of the disk electrode is often hampered by the insulating sheath, which strikes the substrate prematurely due to misalignment of the tip. The protrusion of the active electrode area, like the mercury hemisphere, can allow for an uninhibited approach and a better estimation of the true zero distance. When SECM approach curves are fitted to theory, the zero tip-to-substrate distance and the limiting current of the tip are variable parameters. We have tried to avoid variability in the limiting current by imposing a long equilibration time (minutes) prior to measuring the approach

(41) Wightman, R. M.; Wipf, D. O. In *Electroanalytical Chemistry*; Bard, A. J., Ed.; Marcel Dekker: New York, 1989; Vol. 15, 267.
(42) Bard, A. J.; Fan, F.-R. F.; Kwak, J.; Lev, O. *Anal. Chem*. **1989**, *61*, 132.
(43) Davis, J. M.; Fan, F.-R. F.; Bard, A. J. *J. Electroanal. Chem. Interfacial Electrochem*. **1987**, *238*, 9.

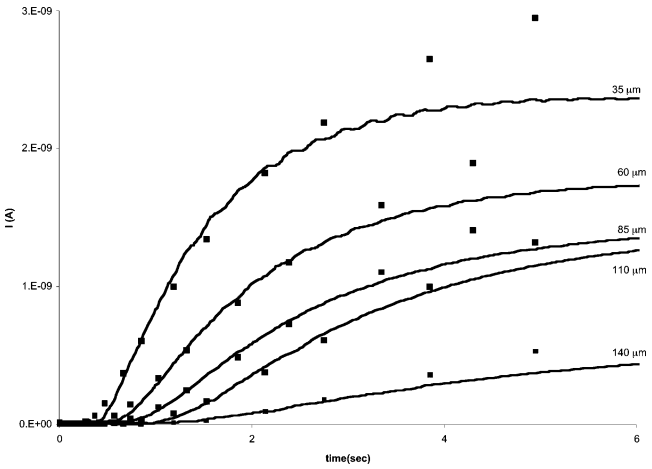

Figure 8. One-parameter fit of the simulated and experimental results for the SG-TC of $TlNO_3$ at a hemispherical Hg/Pt UME for different tip-to-substrate distances. For a 25-μm Hg/Pt UME tip in a 10^{-4} M $TlNO_3$ solution in 0.1 M phosphate buffer at pH 7 with an assumed diffusion coefficient of 1.85×10^{-5} cm^2/s.

curves. The zero distance remains the main uncertainty in fitting the experimental curves to the theory, but the adjustment parameter for a hemispherical tip is minimal.

SG-TC Experiments at a Hemispherical UME. The results for the SG-TC experiments at a hemispherical UME are presented in Figure 8. Unlike the disk experiments, these measurements were performed in the presence of 10^{-4} M $TlNO_3$ in a phosphate buffer solution at pH 7, since this system was of particular interest in studying ionic diffusion through membrane channels[6] and illustrates another feature of the Hg/Pt tip, amalgam formation. Initially the Tl(I) was preconcentrated onto a HMDE by electrochemical formation of an amalgam. The Tl/Hg was then oxidized and the Tl(I) collected at a 25-μm submarine Hg/Pt UME. The tip current, initially at the Tl(I) background level, increases upon collection of the generated Tl(I) and reaches a quasi-steady-state current; it then decreases because of the exhaustion of the substrate (HMDE) amalgam. Figure 8 shows the background-subtracted data and is restricted to the time domain where the amalgam exhaustion was not significant. This was done to simplify the numerical simulation by avoiding the description of the stripping behavior of the amalgamated HMDE. The experiment was repeated for several tip-to-substrate distances that were evaluated from an SECM calibration. From Figure 8, we see that the shorter the distances, the steeper the slope of the transient response, the shorter the diffusion time, and the higher the final steady-state current. Qualitatively the hemispherical transient response is similar to that presented in Figure 5 for the disk UME.

Quantitatively, the response is most sensitive to the tip geometry at small tip-to-substrate separations and short collection times. Indeed, the simulated data for the disk electrode are not a good approximation of the hemispherical response in this regime. The diffusion time is too short and causes an early increase in tip current. The enhanced lateral diffusion of the hemispherical tip reduces the sensitivity of the tip to concentration increases. The diffusion time observed at a hemispherical tip is therefore longer and the slope of the transient is smaller than that of the disk for a given tip-to-substrate separation. This observation concurs with the SECM feedback experiments of (Figure 7b−d) and the work reported by Mandler and co-workers.[7]

The results in Figure 8 show good agreement between experimental and simulated results at a hemispherical tip. The early collection time follows the simulated data very well. The deviation at longer time is explained by the gradual depletion of the Tl amalgam at the substrate. This deviation does not prevent us from extracting good values for the diffusion coefficients for Tl(I) diffusion ($D_s = 1.88 \times 10^{-5}$ cm^2/s). This value is almost identical to the one reported in the literature (1.85×10^{-5} cm^2/s).[44]

CONCLUSIONS

The Hg/Pt UME can be fabricated by two equivalent methods and characterized through optical and electrochemical means. Both techniques agree on the hemispherical nature of the UME and the total coverage of the platinum area by mercury. Voltammetric studies yield reversible results and confirm the extension of the potential window to more negative potentials for SECM in aqueous solutions, allowing mediators such as methyl viologen to be employed. The conducting approach curves for methyl viologen, cobalt sepulchrate trichloride, and hexammineruthenium(III) chloride show good agreement with the hemispherical theory of Mandler et al.[7] Another application of the Hg/Pt electrode is for species such as S-containing peptides that give a good response on a Hg electrode but not at Pt. Recent studies involving glutathione, the major non-protein sulfhydryl present in cells, have been carried out and will be reported elsewhere.[45]

The SECM tip transients in SG-TC mode for a disk and a hemispherical UME were calculated by numerical analysis using PDEase2D, a software program using FEM. The tip transient responses for both geometries were calculated at various tip-to-substrate distances. When the distance is small, the diffusion time is short, the slope of the transient response is large, and the quasi-steady-state current is high. The diffusion times at particular separations were easily approximated by an error function complement relationship. Validation of the numerical analysis was obtained from a comparison of the disk UME response to a large-amplitude potential step in a quiescent solution to that from the expression derived by Shoup and Szabo.[36] The diffusion-limited steady-state current at long collection times also agreed well with the positive feedback theory of SECM. Finally, the extraction of the diffusion coefficient from the numerical analysis correlated well with the experimentally reported values for both geometries.

The electrode geometry affects the transient current response measured in SG-TC experiments. This was confirmed by the numerical simulation and is in line with the feedback studies.[7] But the main advantages of the mercury tips are the enhancement of potential window in the negative potential region and also the protrusion of the hemisphere beyond the glass sheet. The protrusion of the active electrode area can allow for a close approach and actual touching of the metal to the substrate without

(44) Kolthoff, M.; Lingane, J. J. *Polarography*; Interscience Publishers: New York, 1952; p 52.
(45) Mauzeroll, J.; Bard, A. J., unpublished experiments.

problems of premature touching of the glass insulator, thus yielding a better estimation of the true zero distance. Such qualities are desirable in many SECM studies.[6]

ACKNOWLEDGMENT

This work has been supported by the National Science Foundation (CHE 0109587) and the Robert A. Welch Foundation. Dr. M. Buda, Dr. Y. Lee, and Dr. F.-R. F. Fan are acknowledged for their help and useful discussions.

Received for review January 29, 2003. Accepted May 7, 2003.

AC034088L